

# Macrophage-Derived miRNA-Containing Exosomes Induce Peritendinous Fibrosis after Tendon Injury through the miR-21-5p/Smad7 Pathway

Haomin Cui,<sup>1,2,5</sup> Yu He,<sup>3,5</sup> Shuai Chen,<sup>1,5</sup> Deming Zhang,<sup>4</sup> Yaling Yu,<sup>1</sup> and Cunyi Fan<sup>1,2</sup>

<sup>1</sup>Department of Orthopaedics, Shanghai Jiao Tong University Affiliated Sixth People's Hospital, Shanghai 200233, China; <sup>2</sup>Department of Orthopaedics, Shanghai Sixth People's Hospital East Affiliated to Shanghai University of Medicine & Health Sciences, Shanghai 201306, China; <sup>3</sup>Department of Orthopaedics, Peking Union Medical College Hospital, Chinese Academy of Medical Sciences & Peking Union Medical College, Beijing 100010, China; <sup>4</sup>Zhejiang Province's Key Laboratory of 3D Printing and Equipment, College of Mechanical Engineering, Zhejiang University, Hangzhou 310058, China

**Following tendon injury, the development of fibrotic healing response impairs tendon function and restricts tendon motion. Peritendinous tissue fibrosis poses a major clinical problem in hand surgery. Communication between macrophages and tendon cells has a critical role in regulating the tendon-healing process. Yet, the mechanisms employed by macrophages to control peritendinous fibrosis are not fully understood. Here we analyze the role of macrophages in tendon adhesion in mice by pharmacologically depleting them. Such macrophage-depleted mice have less peritendinous fibrosis formation around the injured tendon compared with wild-type littermates. Macrophage-depleted mice restart fibrotic tendon healing by treatment with bone marrow macrophage-derived exosomes. We show that bone marrow macrophages secrete exosomal miR-21-5p that directly targets Smad7, leading to the activation of fibrogenesis in tendon cells. These results demonstrate that intercellular crosstalk between bone marrow macrophages and tendon cells is mediated by macrophage-derived miR-21-5p-containing exosomes that control the fibrotic healing response, providing potential targets for the prevention and treatment of tendon adhesion.**

## INTRODUCTION

Development of the fibrotic healing response is characteristic for musculoskeletal pathologies.<sup>1</sup> Among them, tendinopathy represents a tremendous socioeconomic burden estimated to be \$850 billion per year in health-care costs and indirect lost wage expenditures, according to the American Public Health Association.<sup>2</sup> After injury, tendons commonly heal through peritendinous fibrosis, which does not lead to regeneration of the natural tendon structure but produces adhesions between the tendon and surrounding synovial sheath and impairs tendon gliding, ultimately resulting in tissue stiffness.<sup>3-6</sup> Although multiple strategies have been developed to prevent adhesion formation during tendon healing after injury,<sup>4,7-9</sup> few effective measures that specifically target the pathogenesis of tendon fibrotic disorders are available. Therefore, better understanding of the molecular mechanisms associated with fibrotic healing would promote the

development of effective therapeutic interventions to prevent tendon adhesion.

The healing process in the tendon includes an initial inflammatory phase, when phagocytic monocytes and macrophages migrate to the site of injury. Macrophages are considered players in the onset and perpetuation of tendon disease;<sup>10-12</sup> however, whether they have a positive or passive effect and how they are involved in tendon healing is still a contentious issue. Several studies indicate that macrophages negatively affect the process. Thus, it was reported that macrophage depletion following anterior cruciate ligament reconstruction significantly improved morphological and biomechanical properties at the healing tendon-bone interface, probably because of diminished macrophage-induced transforming growth factor  $\beta$  (TGF- $\beta$ ) production.<sup>13</sup> Macrophage depletion was also shown to reduce cell proliferation and extracellular matrix (ECM) accumulation and ultimately increase the tensile strength of the injured Achilles tendon.<sup>14</sup> On the other hand, it was revealed that nonspecific inhibition of macrophages was detrimental to early ECM formation and ligament strength<sup>15</sup> and that persistence of M1 (proinflammatory) macrophages due to loading positively influenced Achilles tendon regeneration in a rat model.<sup>16</sup> These studies indicate that the functional role of macrophages in the tendon-healing process is controversial and suggest it needs further clarification. Furthermore, specific effects of bone marrow-derived mature macrophages on fibrogenesis in tendon and the underlying mechanisms have not been studied.

Received 5 October 2018; accepted 13 November 2018;  
<https://doi.org/10.1016/j.omtn.2018.11.006>.

<sup>5</sup>These authors contributed equally to this work.

**Correspondence:** Cunyi Fan, Department of Orthopaedics, Shanghai Jiao Tong University Affiliated Sixth People's Hospital, 600 Yishan Road, Shanghai 200233, China.

**E-mail:** [cyfan@sjtu.edu.cn](mailto:cyfan@sjtu.edu.cn)

**Correspondence:** Yaling Yu, Department of Orthopaedics, Shanghai Jiao Tong University Affiliated Sixth People's Hospital, 600 Yishan Road, Shanghai 200233, China.

**E-mail:** [yalingyu@sjtu.edu.cn](mailto:yalingyu@sjtu.edu.cn)



Exosomes are cell-derived membranous vesicles that play an essential role in intercellular communication, both local and systemic, by transferring their cargo to neighboring or distant cell types,<sup>17–19</sup> and exosome-mediated pathways are implicated in multiple pathological processes.<sup>17,20–22</sup> Exosomes contain a variety of microRNAs (miRNAs) emerging as key regulators of cell-cell communication, which play an important role in inflammation, fibrogenesis, and tissue repair when shuttled by exosomes.<sup>21–25</sup> Specific miRNAs have provoked great interest in regard to tendon disorders, including tendon repair and tenocyte development and differentiation.<sup>26</sup> Thus, it was shown that miR-210 accelerated healing of the Achilles tendon in rats through the upregulation of vascular endothelial growth factor (VEGF) and type I collagen.<sup>27</sup> miR-29b, which is the most widely studied miRNA in the tendon, has been reported to improve tendon healing, reduce adhesion formation after injury, and accelerate tenogenic differentiation by down-regulating TGF- $\beta$ 1/Smad3 signaling.<sup>28,29</sup> Recently, Watts and colleagues<sup>30</sup> proposed that miR-29a replacement may be used as a therapeutic tool to improve tendon repair after injury through targeting interleukin 33 (IL-33) expression and collagen type III synthesis.<sup>1</sup>

These findings signify a novel approach to molecular therapies of tendon diseases. However, there is still a lack of mechanistic understanding of miRNAs' function in the tendon compared to other tissues, which precludes the advancement of miRNAs into clinical practice. The latest systematic review summarizes the effects of 14 tendon-specific miRNAs on tendon tissue repair.<sup>31</sup> Among them, miRNAs showing aberrant expression during fibrogenesis (fibro-miRNAs), including miR-21, have attracted considerable attention as a potential approach in the development of new anti-fibrotic therapies.<sup>32</sup> Thus, it was reported that miR-21 inhibition attenuated fibrosis in the kidney,<sup>33</sup> heart,<sup>34</sup> lung,<sup>35</sup> and skeletal muscle.<sup>36</sup> However, it is unclear how the regulatory function of tendon-related miRNAs, such as miR-21, and their targets are finely orchestrated in the formation of tendon adhesion. Currently, most data on miRNA-mediated mechanisms in tendon disease are based on the use of unpackaged miRNAs, whereas little is known about the effects of miRNAs existing as cargo of macrophage exosomes.

In this study, our results indicated that macrophage-derived exosomal miR-21-5p leads to increased proliferation, migration, and fibrotic activity of tendon cells via targeting Smad7. These findings provide new insight into the role of exosomal miRNAs secreted by macrophages in tendon adhesion.

## RESULTS

### Macrophages Are Necessary for Peritendinous Fibrosis Formation

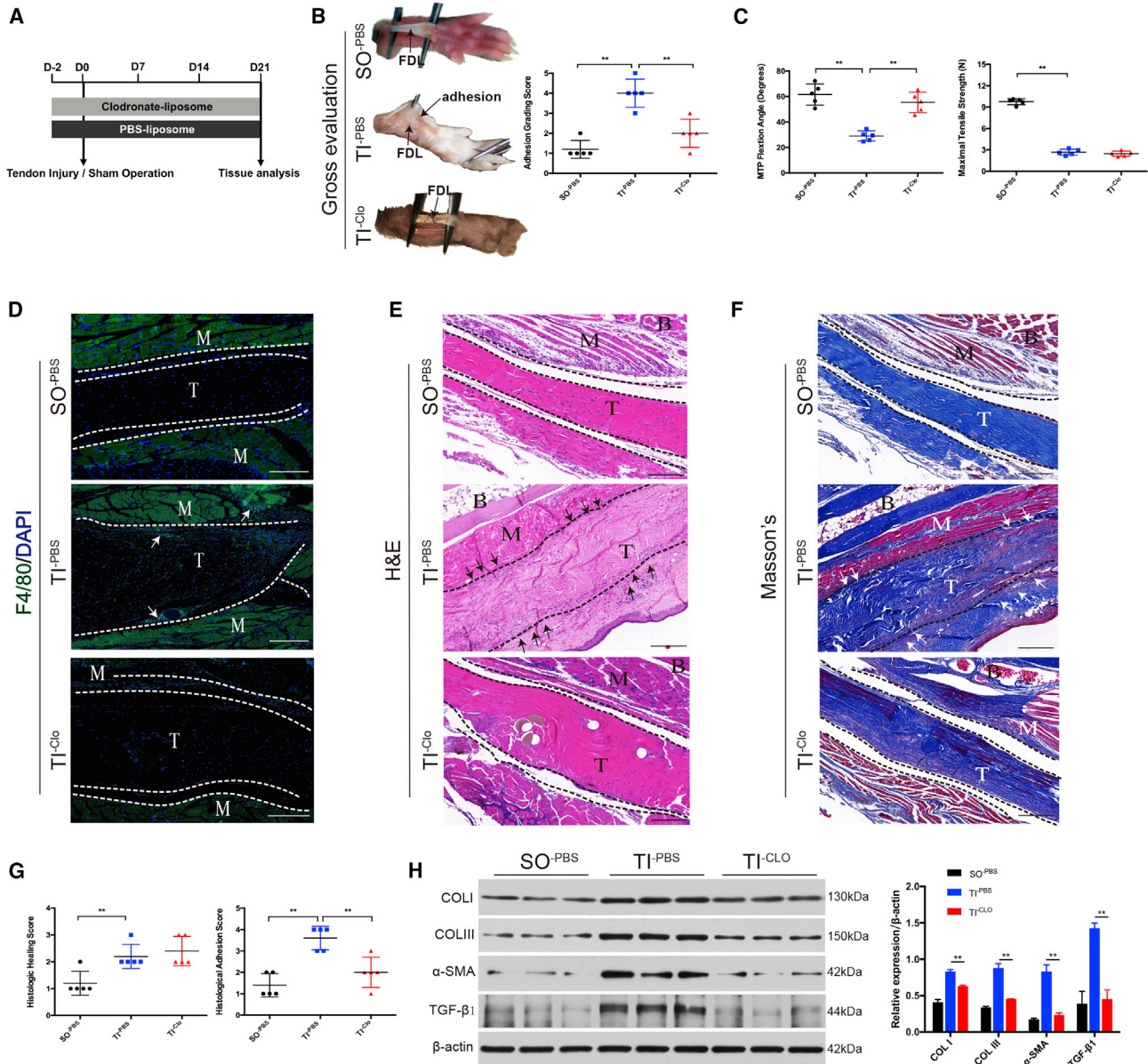
To assess the role of bone marrow-derived macrophages (BMDMs) in peritendinous fibrosis following tendon injury, macrophages were depleted with Clo-Lipo 2 days prior to and immediately before tendon surgery (days  $-2$  and  $0$ , respectively) and at days  $7$ ,  $14$ , and

$21$  after tendon injury, whereas the control group received PBS-containing liposomes (PBS-Lipo) (Figure 1A). Mice were randomly assigned to the following three groups: sham operation (SO) with PBS-Lipo treatment (SO<sup>-PBS</sup>), flexor digitorum longus (FDL) tendon injury (TI) with PBS-Lipo treatment (TI<sup>-PBS</sup>), and FDL TI with Clo-Lipo treatment (TI<sup>-Clo</sup>). The mice were evaluated for peritendinous adhesion severity at 3 weeks post-operation. The results revealed that, in the SO<sup>-PBS</sup> group, the tendon surface was smooth and no obvious tendon adhesion was observed, whereas, in the TI<sup>-PBS</sup> group, there was severe tendon adhesion with extensive connective and fibrotic tissue formation around the tendon repair area, which required sharp dissection for separation, and, in the TI<sup>-Clo</sup> group, only little fibrous tissue around the tendon repair area was present. Consistent with these observations, the adhesion grading score was significantly higher in the TI<sup>-PBS</sup> group than in the SO<sup>-PBS</sup> and TI<sup>-Clo</sup> groups (Figure 1B).

To assess adhesion formation, we measured the metatarsophalangeal (MTP) joint flexion range of motion (ROM). Compared with the SO<sup>-PBS</sup> group, there was a significant decrease of the MTP joint ROM in the TI<sup>-PBS</sup> group, which was rescued in the TI<sup>-Clo</sup> group (Figure 1C), indicating that macrophage depletion effectively alleviated peritendinous fibrosis and suggesting a role of macrophages in the development of tendon adhesion. Immediately following assessment of the MTP joint flexion, the tendons were harvested to measure the tensile strength. There was no significant difference between the TI<sup>-PBS</sup> and TI<sup>-Clo</sup> groups in the maximal tensile strength (Figure 1C). Theoretically, a greater quantity of fibrous tissue improves the strength of repaired tendon to a certain extent; however, such an improvement is limited. The closer apposition of broken ends of tendon in the macrophage-depleted mice (due to less fibrous tissue between two breaks) may allow for continued development of collagen fiber continuity, thus neutralizing the weakened strength caused by less fibrous tissue formation.

The efficacy of macrophage depletion by clodronate liposomes was confirmed by immunohistochemistry (Figure 1D). In the SO<sup>-PBS</sup> group, the demarcation line between flexor tendons and surrounding tissues barely contained macrophage marker F4/80-positive cells, suggesting the absence of fibrogenesis, whereas, in the TI<sup>-PBS</sup> group, many cell nuclei and F4/80-positive cells were observed between the injured tendon and surrounding tissue, indicating adhesion formation. However, in the TI<sup>-Clo</sup> group, there were hardly any F4/80-positive cells, and the line between the injured tendon and surrounding tissue reappeared, indicating that fibrous adhesions were not developed.

Histological analysis showed that injured tendons in the TI<sup>-Clo</sup> group exhibited reduced adhesion formation and had fewer infiltrated inflammatory cells compared to the TI<sup>-PBS</sup> group (Figures 1E and 1F). Consistent with these results, the histological adhesion score was higher in the TI<sup>-PBS</sup> group than in the TI<sup>-Clo</sup> group, indicating decreased fibrogenesis in the latter; however, no difference was observed in the histological tendon-healing score between these



groups (Figure 1G). These data showed that macrophage depletion reduced tendon fibrogenesis.

Peritendinous fibrosis is manifested by the excessive accumulation of ECM components collagen type I (COL I), COL III, and alpha-smooth muscle actin ( $\alpha$ -SMA) in the injured tendon.<sup>8</sup> The expression

of  $\alpha$ -SMA is often used as an additional phenotypic and diagnostic marker of myofibroblasts in fibrotic tissue.<sup>37</sup> TGF- $\beta$ 1 is also considered to be associated with the formation of adhesions around healing digital flexor tendons.<sup>38</sup> Therefore, we assessed the expression of these pro-fibrotic markers in repaired tendons by western blotting. The results showed the levels of COL I, COL III,  $\alpha$ -SMA, and TGF- $\beta$ 1 were



significantly increased in the TI<sup>PBS</sup> group compared with those in the SO<sup>PBS</sup> group, but then significantly decreased after macrophage depletion in the TI<sup>ClO</sup> group (Figure 1H).

Overall, these data indicate that macrophages are required for adhesion formation after tendon injury.

### Characterization of Macrophage-Derived Exosomes and Internalization

To determine whether macrophages can secrete exosomes, we isolated BMDMs and cultured them for 72 hr. Electron microscopy and nanoparticle-tracking analysis (NTA) revealed abundant BMDM-derived exosomes with a diameter of 70–150 nm (Figures 2A and 2B). With the exception of showing macrophage marker CD68 in macrophages, western blotting analysis showed that these vesicles were positive for exosome-specific markers CD9, TSG101, CD63, and ALIX (Figure 2C), confirming that they primarily represented exosomes, the production of which from BMDMs was decreased by the exosome secretion inhibitor GW4869 (Figure 2D).

Then, we demonstrated that macrophages could secrete extracellular miRNAs, which were then transported into target cells. Because miR-223 is a myeloid cell-specific miRNA,<sup>39</sup> we transfected BMDMs with a Cy3-labeled miR-223 mimic and co-cultured them with fibroblasts and tenocytes in Transwell plates (Figure 2E). The appearance of Cy3-positive cells in the lower chamber indicated that the Cy3-miR-223 mimic was transferred into target cells in the lower chamber from the transfected BMDMs in the upper chamber, presumably by exosomes. Compared with the recipient fibroblasts or tenocytes seeded in the lower well without co-culture, an increased expression of miR-223 in the recipient cells was observed after co-culture.

To determine whether BMDM-derived exosomes could be taken up by tenocytes and fibroblasts, exosomes were labeled with a fluorescent dye, PKH67, and added to tenocyte or fibroblast cultures for different times. After incubation, fluorescence microscope imaging showed the presence of PKH67 spots in recipient fibroblasts, suggesting that labeled exosomes released by BMDMs were delivered to fibroblasts and tenocytes (Figure 2F).

Cumulatively, these findings suggest that macrophages could secrete exosomes, which were taken up by fibroblasts and tenocytes.

### Macrophage-Derived Exosomes Promote Proliferation, Migration, and Fibrotic Activity of Tendon Cells *In Vitro*

Extreme cell proliferation and migration, persistent myofibroblast activation, as well as upregulated expression of pro-fibrotic cytokines and ECM proteins are involved in the progression of fibrotic diseases, including tendon adhesion.<sup>8,9,37</sup> As fibroblasts and tenocytes, which are the principal cell types of the tendon and play a key role in the pathogenesis of tendon adhesion,<sup>8,9</sup> demonstrated the uptake of BMDM-secreted exosomes, we examined whether it affected their proliferation. The results indicated that the treatment of fibroblasts

with BMDM exosomes promoted their proliferation (Figure 3A) and significantly accelerated migration (Figure 3B). Furthermore, the expressions of COL I, COL III,  $\alpha$ -SMA, and TGF- $\beta$ 1 were upregulated both at the mRNA and protein levels in fibroblasts treated with BMDM exosomes, as evidenced by real-time qPCR (Figure 3C) and immunocytochemistry (Figure 3D) analyses.

Similar results were obtained in tenocytes, which also demonstrated increased proliferation and migration (Figures 3E and 3F) and expression of pro-fibrotic proteins (Figures 3G and 3H) following BMDM-exosome treatment.

These results suggest that BMDM exosomes may modulate tendon adhesion by regulating proliferation, migration, and fibrogenesis of fibroblasts and tenocytes.

### Macrophage-Derived Exosomes Induce Peritendinous Fibrosis after Tendon Injury *In Vivo*

As exosomes can enter the circulation and act distantly, we tested whether BMDM-derived exosomes could penetrate the injured tendon and modulate tendon adhesion *in vivo*. For this, we injected macrophage-depleted mice intravenously with PKH67-labeled BMDM exosomes, and the labeled exosomes were tracked in frozen sections from the heart, lungs, liver, spleen, muscle, adipose, and both FDL tendons. The PKH67 signal was evident in the spleen, but it was rather weak in the liver, kidney, and muscle, and it was not observed in adipose and cardiac tissues or the lungs (Figure 4A), indicating low or no exosome transfer. However, a more significant presence of fluorescently labeled exosomes was observed in the TI side compared to the SO side or the other uninjured tissues (Figures 4B and 4C), suggesting that BMDM exosomes preferably migrate to the injured tendon, similar to the macrophage accumulation in the healing region, where they regulate the tendon-healing process.

To quantitatively evaluate the effect of BMDM exosomes on tissue-specific responses in the injured tendon, macrophage-depleted mice were intravenously injected with 20  $\mu$ g BMDM exosomes or empty liposomes (control) every 3 days (Figure 5A). After 21 days, dense fibrotic tissue requiring sharp dissection for separation from the tendon was observed in the BMDM-exosome group, in contrast to the smooth tendon surface that was observed in the control group (Figure 5B). The administration of BMDM exosomes significantly increased fibrogenesis around the injured tendon, as evidenced by a higher adhesion grading score and lower MTP joint flexion ROM compared to the control (Figure 5C). In addition, histological results indicated that treatment with BMDM exosomes led to severe adhesion formation between the tendon and surrounding tissue, whereas a clear boundary was evident between the tendon and surrounding tissue in the control group (Figures 5D and 5E), which also had a significantly lower histological adhesion score (Figure 5F). However, no difference was found between the two groups in tendon healing according to the histological tendon-healing score (Figure 5F), which was consistent with the data on biomechanical strength. These

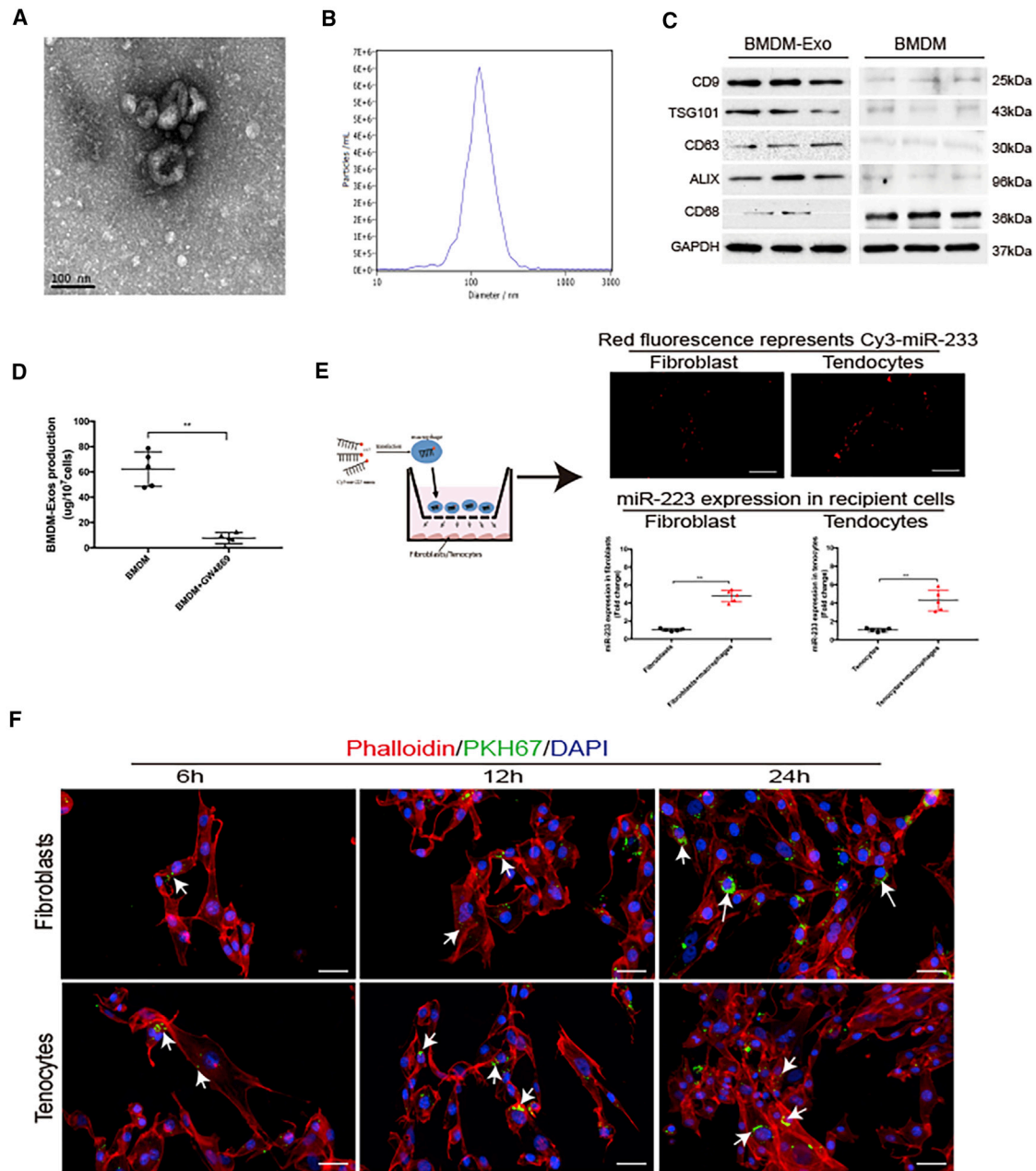


**Figure 2. Characteristics of BMDM-Derived Exosomes and Internalization**

(A) Representative electron microscopy pictures for exosomes secreted by BMDM. Scale bar, 100 nm. (B) Size of exosomes was measured by NTA. (C) Western blotting analysis of exosome markers CD9, TSG101, CD63, ALIX and macrophage marker CD68 ( $n = 3$  per group). (D) Exosome production by macrophages. The data are shown as the mean  $\pm$  SD ( $n = 5$  per group). (E) BMDMs transfected with a Cy3-labeled miR-223 mimic were co-cultured with tenocytes or fibroblasts in a transwell, and the expression levels of miR-223 in tenocytes or fibroblasts are shown ( $n = 5$  per group). Scale bars, 20  $\mu$ m. (F) Representative immunofluorescence images showing the internalization of PKH67-labeled BMDM-derived exosomes (green) by fibroblasts or tenocytes stained with phalloidine (red) at 6, 12, and 24 hr. Cell nuclei were stained with DAPI (blue). White arrows indicate exosomes (green). Scale bars, 100  $\mu$ m. \* $p < 0.05$  and \*\* $p < 0.01$ .

findings indicated that BMDM exosomes induced fibrogenesis around the injured tendon without affecting its mechanical strength. In agreement with these results, the fibrotic process was enhanced in

the BMDM-exosome group compared with that in the control group, as evidenced by the increased expression of COL I, COL III,  $\alpha$ -SMA, and TGF- $\beta$ 1 (Figure 5G).

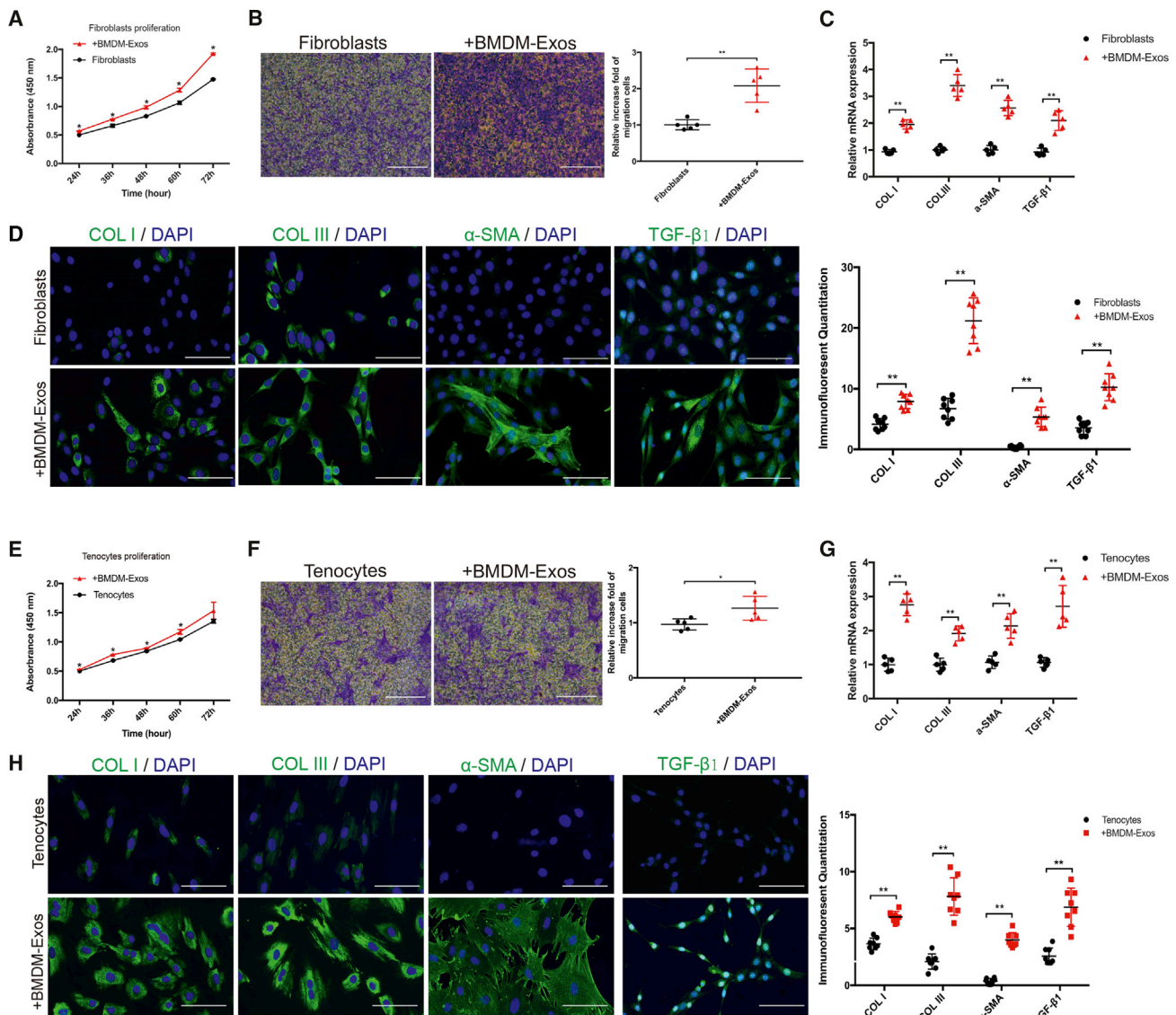


**Figure 3. BMDM-Derived Exosomes Promote Proliferation, Migration, and Fibrotic Activity of Fibroblasts and Tenocytes**

(A) Proliferation of fibroblasts treated with or without BMDM exosomes (n = 5 per group). (B) Migration and quantification of migrating fibroblasts (n = 5 per group). Scale bars, 100  $\mu$ m. (C) mRNA expression of COL I, COL III,  $\alpha$ -SMA, and TGF- $\beta$ 1 in fibroblasts (n = 3 per group). (D) Representative immunofluorescence images and quantification of COL I, COL III,  $\alpha$ -SMA, and TGF- $\beta$ 1 protein expression in fibroblasts (n = 8 per group). Scale bars, 50  $\mu$ m. (E) Proliferation of tenocytes treated with or without BMDM exosomes (n = 5 per group). (F) Migration and quantification of migrating tenocytes (n = 5 per group). Scale bars, 100  $\mu$ m. (G) mRNA expression of COL I, COL III,  $\alpha$ -SMA, and TGF- $\beta$ 1 in tenocytes (n = 5 per group). (H) Representative immunofluorescence images and quantification of COL I, COL III,  $\alpha$ -SMA, and TGF- $\beta$ 1 protein expression in tenocytes (n = 8 per group). Scale bars, 50  $\mu$ m.

\*p < 0.05 and \*\*p < 0.01.

Thus, these data indicate that BMDM-derived exosomes can migrate into the injured tendon and induce fibrotic healing.

#### Macrophage-Derived Exosomes Shuttle miR-21-5p

Exosomes are intriguing as signaling intermediates with cargo rich in miRNA molecules.<sup>40</sup> To further explore the mechanisms underlying stimulation of tendon adhesion by BMDM exosomes, we investigated

exosomal miRNA profiles using high-throughput miRNA sequencing. Among the identified miRNAs, miR-21-5p, which has been previously reported to promote fibrogenesis in cardiac tissue<sup>41</sup> and the kidney,<sup>42</sup> showed the highest abundance (Figure 6A). Furthermore, the miR-21-5p presence was significantly increased in tenocytes and fibroblasts after co-culture with BMDMs; however, 24-hr pre-treatment of BMDMs with GW4869, which inhibited



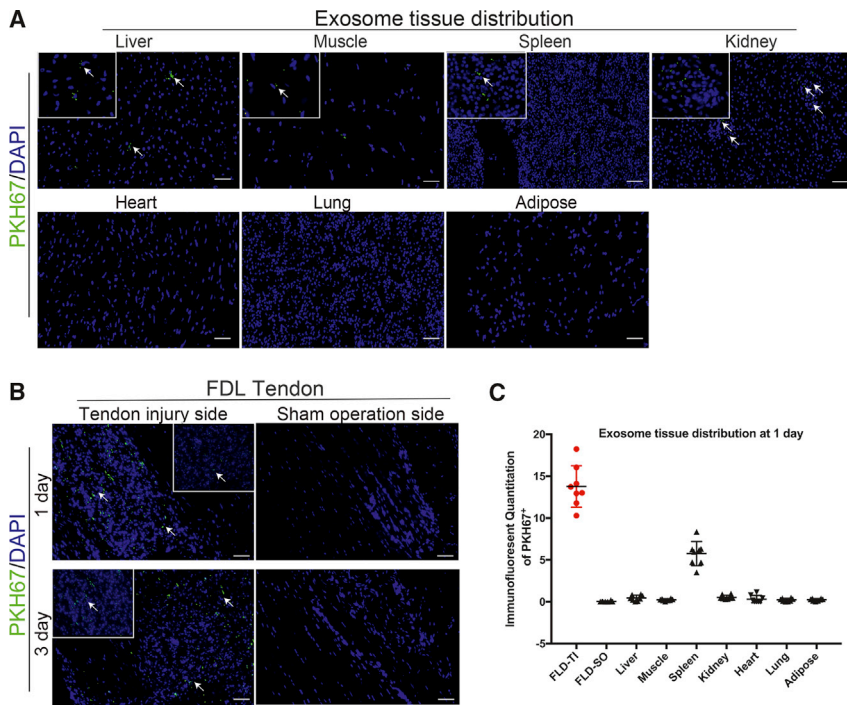


**Figure 4. Distribution of BMDM-Derived Exosomes in Tissues of Mice with Tendon Injury**

(A) Representative immunofluorescence images of PKH67-labeled exosomes (arrows) in the liver, muscle, spleen, and kidney of recipient mice 1 day after intravenous injection of BMDM exosome. (B) Representative immunofluorescence images of PKH67-labeled exosomes (arrows) in the TI side and SO sides of recipient mice 1 and 3 days after BMDM-exosome administration. (C) Quantitative fluorescence of exosome distribution at 1 day after administration ( $n = 8$  per group). \* $p < 0.05$  and \*\* $p < 0.01$ .

exosome production, reduced miR-21 delivery to tenocytes and fibroblasts (Figures 6B and 6C), indicating that the secretion of extracellular miRNAs by macrophages occurs mainly through exosomes.

We also performed *in vivo* experiments to determine whether peritendinous fibrosis was associated with abnormal miR-21-5p levels and whether treatment with BMDM exosomes led to miR-21-5p accumulation in the injured tendon. Our results showed that the level of miR-21-5p, which was relatively low in tendon cells following SO, was significantly upregulated in peritendinous fibrotic tissue 21 days after tendon injury (Figure 6D). Macrophage-depleted TI mice had decreased miR-21-5p levels in the tendon, which corresponded to fibrous tissue formation, whereas the treatment of these mice with BMDM exosomes led to miR-21-5p accumulation in peritendinous fibrotic tissue (Figure 6E).

Taken together, these results suggest that the delivery of exosomal miR-21-5p contributes to macrophage communication with tenocytes and fibroblasts and may promote peritendinous fibrosis after tendon injury.

#### miR-21-5p Promotes Proliferation, Migration, and Fibrotic Activity of Tendon Cells *In Vitro*

To define the effect of increased intracellular miR-21-5p on tendon cells, we transfected fibroblasts and tenocytes with either fluorescently labeled miR-21-5p mimic or control miRNA termed miRNA-mimic negative control (NC) (Figures 7A and 7B). Fibroblast and tenocyte transfection with miR-21-5p mimic produced more than a 90% efficiency in each cell, and it resulted in significantly increased

miR-21-5p expression compared to controls. Transfection with miRNA-mimic NC exhibited the same efficacy as miR-21-5p mimic, but, as expected, it did not result in increased expression of miR-21-5p.

Subsequent analysis of proliferation and migration in miR-21-5p-transfected fibroblasts and tenocytes revealed a significant upregulation of proliferation capacity (Figures 7E and 7F) and migration capacity (Figures 7G and 7H)

compared to control transfection. Furthermore, miR-21-5p transfection upregulated the expression of COL I, COL III,  $\alpha$ -SMA, and TGF- $\beta$ 1 in fibroblasts and tenocytes, both at the mRNA (Figures 7G and 7H) and protein (Figures 7I and 7J) levels.

These *in vitro* transfection data support evidence for a pro-fibrogenic role of miR-21-5p in tendon tissue by showing that an increase in intracellular miR-21-5p stimulated fibroblasts and tenocytes to differentiate into myofibroblasts (overexpression of  $\alpha$ -SMA) and overproduce ECM markers and fibrogenic markers.

#### miR-21-5p Promotes Proliferation, Migration, and Fibrotic Activity of Tendon Cells by Inhibiting the Expression of Smad7

To explore how miR-21-5p exerts its function in tendon cells, we used Kyoto Encyclopedia of Genes and Genomes (KEGG) and Ingenuity Pathway Analysis to predict target genes of miR-21-5p. Then, Smad7 was identified as a potential target of miR-21-5p, which has been proven to play an important role in renal fibrosis.<sup>42</sup> RT-PCR and western blot were used to investigate how miR-21-5p influences Smad7. RT-PCR assays revealed that miR-21-5p mimic-transfected fibroblasts and tenocytes exhibited decreased Smad7 mRNA levels (Figures 8A and 8B), and western blot assays revealed that miR-21-5p mimic-transfected fibroblasts and tenocytes displayed decreased Smad7 protein levels (Figures 7C and 7D) These data demonstrated that miR-21-5p suppresses Smad7 protein expression by degrading the corresponding mRNA.

Although the results above revealed that Smad7 was a target of miR-21-5p, whether miR-21-5p promoted fibrogenesis of tendon cells via mediating Smad7 expression remains mixed. Therefore,

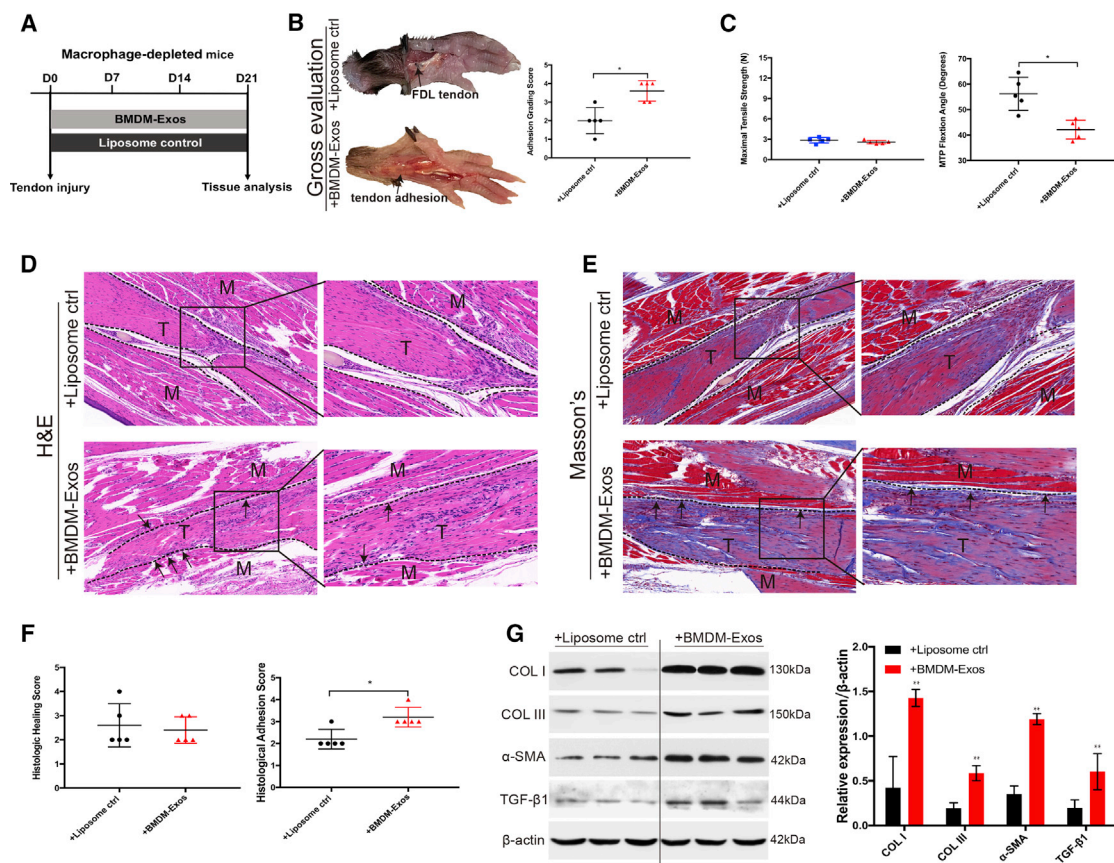


**Figure 5. BMDM-Derived Exosomes Induce Peritendinous Fibrosis *In Vivo***

(A) Experimental design scheme showing treatment of macrophage-depleted mice with BMDM exosomes or empty liposomes (control). (B) Macroscopic images of tendons after the treatment with control liposomes or BMDM exosomes and adhesion grading score (n = 5 per group). (C) Maximal tensile strength and MTP joint flexion ROM (n = 5 per group). (D and E) Histology of adhesion. T, tendon; M, muscle; B, bone. Arrows indicate tendon adhesion in (D) H&E and (E) Masson staining. Dotted lines indicate the border of FDL tendon or surrounding tissue. Scale bars, 100  $\mu$ m. (F) Histological adhesion score and histological healing score (n = 5 per group). (G) Western blot analysis and quantification of the levels of COL I, COL III,  $\alpha$ -SMA, and TGF- $\beta$ 1 expression (n = 3 per group). \*p < 0.05 and \*\*p < 0.01.

we used lentiviral vectors LV-Smad7 to transfect fibroblasts and tenocytes that had been transfected with miR-21-5p mimics. Proliferation assay (Figures 8E and 8F) and migration assay (Figures 8G and 8H) revealed that LV-Smad7 effectively counteracted the increase in proliferation and migration abilities resulting from miR-21-5p overexpression in fibroblasts and tenocytes. Furthermore, western blot assay results indicated that Smad7 and ECM protein and fibrosis protein levels were reversed in the miR-21-5p mimic + LV-Smad7 group relative to miR-21-5p mimics (Figure 8I).

Collectively, our findings confirmed the hypothesis that miR-21-5p promotes fibrogenesis of tendon cells by inhibiting the expression of Smad7. Overall, our results indicate that BMDM exosomes containing miRNA, such as miR-21-5p, can be transported to the injured tendons and induce fibrous tissue formation by regulating the functional activity of fibroblasts and tenocytes in response to tendon injury (Figure 8J).

## DISCUSSION

Exosomal miRNAs have emerged as key regulators of multitudinous cellular processes with fundamental roles in disease and tissue repair.<sup>22,24,43</sup> In a new era of molecular therapies, miRNA interference is deemed as a promising approach to treat tendinopathy as well as other disorders affecting musculoskeletal soft tissues.<sup>26</sup> In this study based on a mouse model of tendon adhesion, we showed that macrophage-derived miRNA-containing exosomes had a significant effect on the development of peritendinous fibrosis. We also revealed a previously unreported role of exosomal miR-21-5p in the complex biological processes involved in the formation of tendon adhesion.

Inflammatory macrophages are undoubtedly relevant to tendon damage, and they have recently become increasingly associated with tendon pathologies.<sup>16</sup> It is established that macrophages contribute to the initiation of tendon pathology by releasing inflammatory cytokines, such as IL-6 and tumor necrosis factor alpha (TNF- $\alpha$ ).<sup>44</sup> Surgically induced tendon injury elicited an increase in macrophage



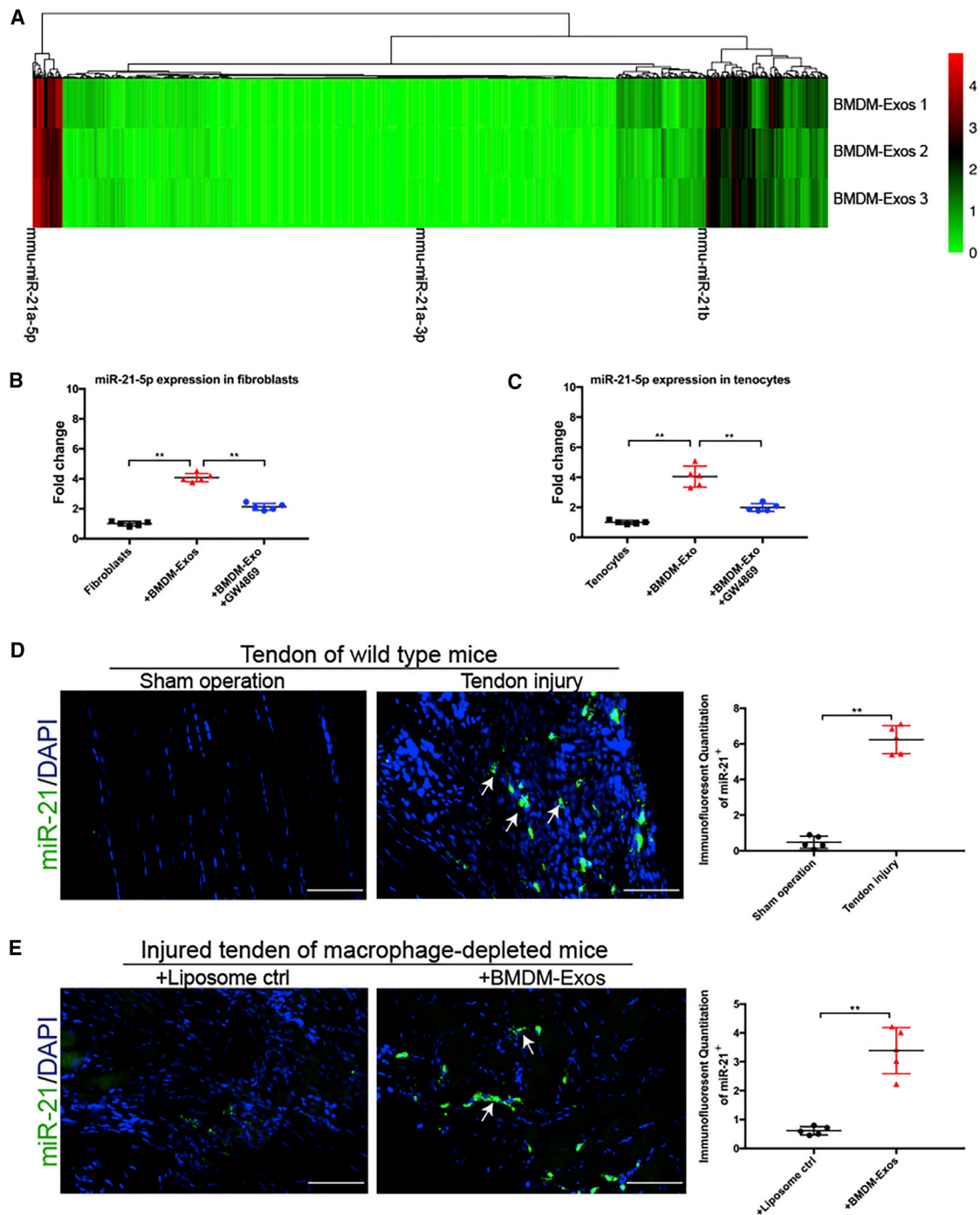


**Figure 6. miR-21-5p Is a Predominant miRNA Component in BMDM Exosomes**

(A) Heatmap diagram of miRNA content in exosomal cargo, indicating high abundance of miR-21-5p in BMDM exosomes (n = 3 per group). Red, high expression; green, low expression. (B and C) Fibroblasts (B) and tenocytes (C) were treated with BMDM exosomes for 24 hr and analyzed for miR-21a-5p levels by real-time qPCR (n = 5 per group). (D) Representative fluorescence in situ hybridization (FISH) images and fluorescence quantitation of miR-21-5p expression in tendon of wild type mice (n = 5 per group). Scale bars, 100  $\mu$ m. (E) Representative FISH images and fluorescence quantification of miR-21 expression in tendon of macrophage-depleted mice (n = 5 per group). Scale bars, 100  $\mu$ m. \*p < 0.05 and \*\*p < 0.01.

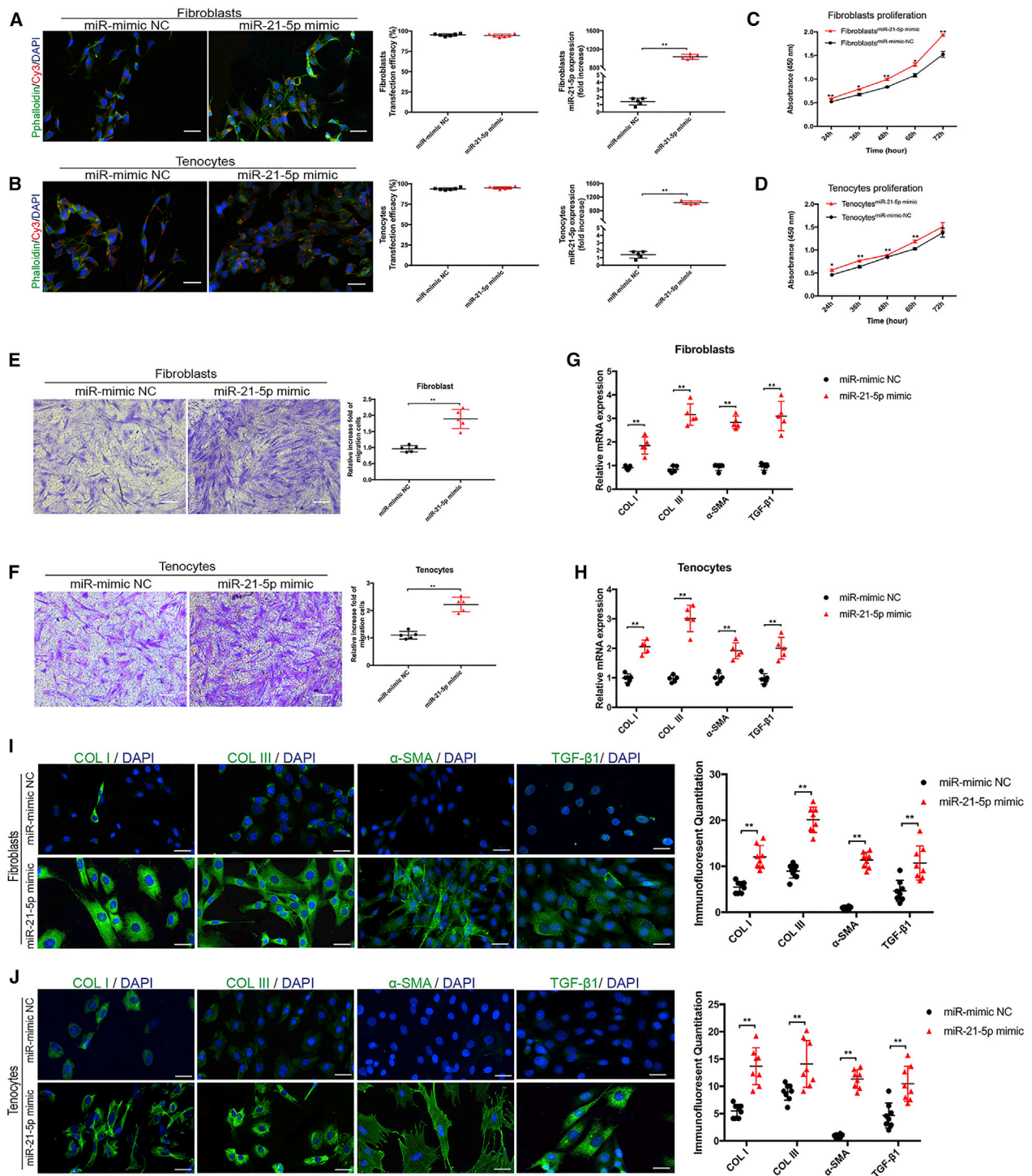


**Figure 7. miR-21-5p Promotes Proliferation, Migration, and Pro-fibrotic Activities of Fibroblasts and Tenocytes In Vitro**

(A and B) Representative immunofluorescence images, transfection efficacy, and qPCR of (A) fibroblasts and (B) tenocytes transfected with Cy3-labeled miR-21-5p mimic or miRNA-mimic NC for 48 hr (n = 5 per group). Scale bars, 100  $\mu$ m. (C and D) Proliferation of (C) fibroblasts and (D) tenocytes (n = 5 per group). (E and F) Migration and quantification of migrating (E) fibroblasts and (F) tenocytes (n = 5 per group). Scale bars, 100  $\mu$ m. (G and H) mRNA expression of COL I, COL III,  $\alpha$ -SMA, and TGF- $\beta$ 1 in (G) fibroblasts and (H) tenocytes (n = 5 per group). (I and J) Representative immunofluorescence images and quantification of COL I, COL III,  $\alpha$ -SMA, and TGF- $\beta$ 1 protein expression in (I) fibroblasts and (J) tenocytes (n = 8 per group). Scale bars, 50  $\mu$ m. \*p < 0.05 and \*\*p < 0.01.

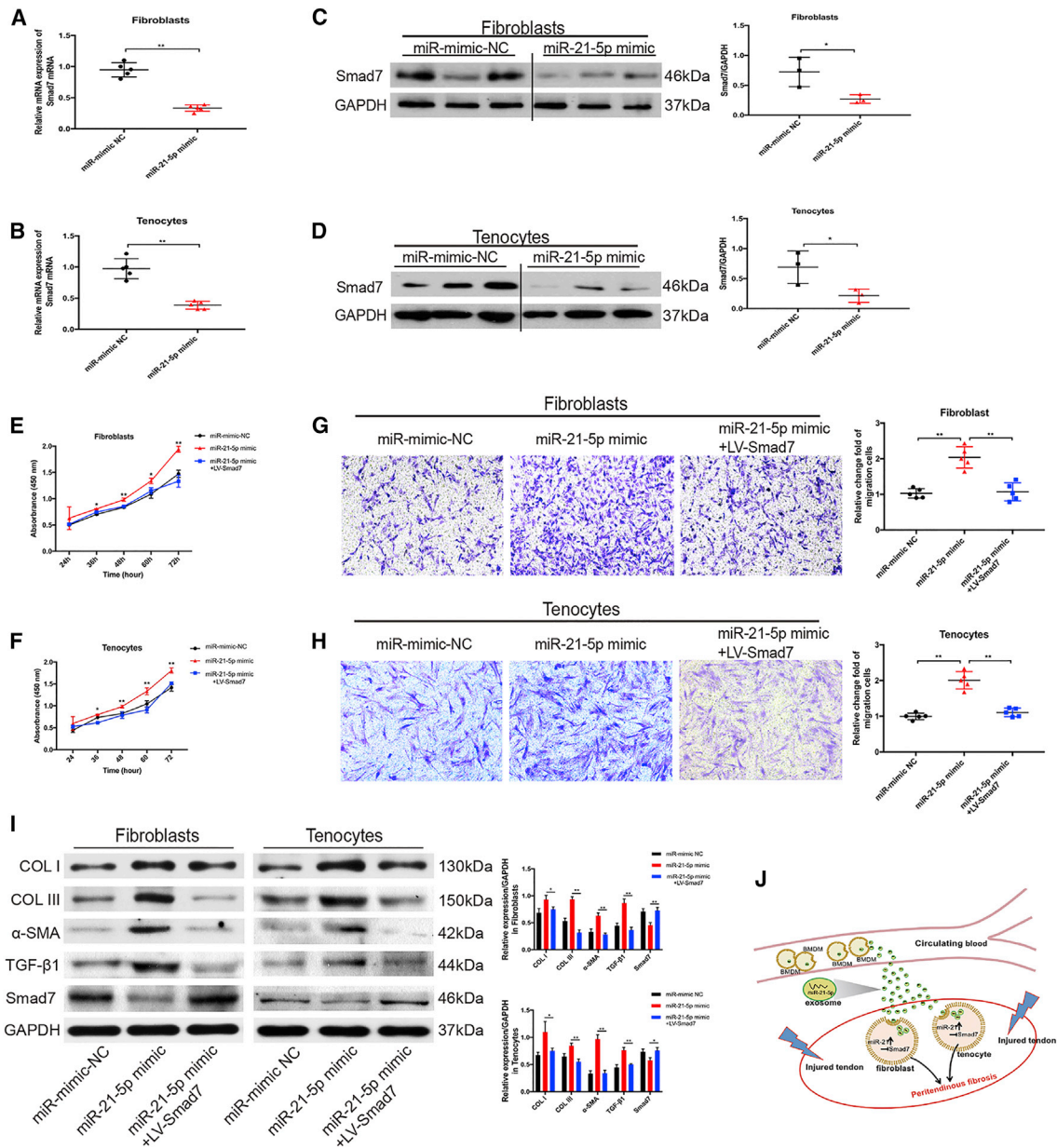


**Figure 8. miR-21-5p Promotes Proliferation, Migration, and Pro-fibrotic Activities of Fibroblasts and Tenocytes by Targeting Smad7**

(A and B) mRNA expression of Smad7 in (A) fibroblasts and (B) tenocytes transfected with miRNA-mimic NC or miR-21-5p mimic (n = 5 per group). (C and D) Western blot analysis and quantification of the levels of Smad7 expression in (C) fibroblasts and (D) tenocytes transfected with miRNA-mimic NC or miR-21-5p mimic (n = 3 per group). (E and F) Proliferation of (E) fibroblasts and (F) tenocytes transfected with miRNA-mimic NC, miR-21-5p mimic, or miR-21-5p mimic + LV-Smad7, respectively (n = 5 per group). (G and H) Migration and quantification of migrating (G) fibroblasts and (H) tenocytes (n = 5 per group). Scale bars, 100  $\mu$ m. (I) Western blot analysis and quantification of the levels of COL I, COL III,  $\alpha$ -SMA, TGF- $\beta$ 1, and Smad7 expression (n = 3 per group). (J) Proposed schematic diagram of BMDM-derived exosomal miR-21-5p mediating peritendinous fibrosis after tendon injury. \*p < 0.05 and \*\*p < 0.01.

infiltration between 1 and 28 days post-injury in a rat model of Achilles tendon injury.<sup>45</sup> Additionally, in one study involving human tendinopathy, an increasing infiltration of macrophages was observed in torn supraspinatus tendon.<sup>44</sup> But, there is no clear picture of the influence of macrophages on tendon healing. Several researchers

have reported that macrophage depletion is related to improved quality of the healing tissue,<sup>13,14</sup> while others have reported that macrophage depletion results in unfavorable healing.<sup>16</sup> Moreover, although macrophages regulate tendon pathology by means of releasing cytokines or directly migrating to the region, whether there



are any other regulatory mechanism, such as exosomes, mediating distant macrophage-tendon cell communication is not known.

To establish the role of macrophages in tendon adhesion in mice, we used a mouse model where the macrophage is pharmacologically depleted. Such macrophage-depleted mice have less peritendinous fibrosis formation around the injured tendon compared with wild-type littermates. Macrophage-depleted mice restart fibrotic tendon healing by treatment with bone marrow macrophage-derived exosomes. This enabled us to identify exosomes that are derived from macrophages able to induce the fibrotic healing process. Our data also suggested that macrophage-derived exosomes could penetrate the injured tendon independently of infiltrating macrophages themselves. The significantly lower abundance of BMDM exosomes in normal tissues may be attributed to traumatic inflammatory response, which increases the accumulation of macrophage exosomes to the injured site.<sup>46</sup> In this study, we found that BMDM exosomes promote the proliferation and migration abilities of tenocytes and fibroblasts and pro-fibrotic activity around the repaired tendon, suggesting that BMDM exosomes are important components of the peritendinous microenvironment, where they act as important messengers mediating intercellular crosstalk.

miRNAs have been shown to regulate tenocyte differentiation and the development of tendinopathy,<sup>27,31</sup> including collagen expression and the release of inflammatory mediators.<sup>1,47</sup> Thus, it was shown that miR-124 inhibited collagen expression of human tendon-derived stem cells.<sup>48</sup> Previous studies raise an intriguing possibility that miRNA targeting could offer a therapeutic approach to tendon injury repair. The miR-29 family is the most widely studied in regard to tendon disorders;<sup>1,28,29</sup> however, in this study, we provide evidence of the functional role of a single miRNA, miR-21-5p, in the development of tendon adhesion. Several previous reports indicated that the expression of collagens and other ECM components is controlled by miR-21,<sup>36,41,42</sup> which in turn is upregulated by TGF- $\beta$ 1 in several pathological conditions.<sup>34,49</sup> Although TGF- $\beta$ 1 plays an important role in mediating the increased expression of miR-21, there are other yet unknown mechanisms responsible for the increased expression of miR-21.<sup>35</sup> In this study, we demonstrated that miR-21a-5p was significantly enriched in BMDM-derived exosomes and could be transferred into tenocytes and fibroblasts, which would be then transformed into pro-fibrotic myofibroblasts, as evidenced by the upregulation of  $\alpha$ -SMA expression. Thus, our data broaden the perspective of the mechanism of miR-21-5p overexpression in tendon, and they reveal that exosomal miR-21-5p acts as a critical inducer of pro-fibrotic protein expression in peritendinous fibrosis.

To further investigate the mechanisms underlying miR-21-5p-induced fibrogenesis in tenocytes, we chose Smad7 as a candidate gene because of its close involvement in inflammation and fibrosis.<sup>35,36,50,51</sup> Previous studies have demonstrated that TGF- $\beta$ 1/SMAD signaling contributes to the formation of adhesions around healing digital flexor tendons<sup>9,52</sup> and that blocking of the TGF- $\beta$ 1 pathway could prevent the formation of tendon adhesions.<sup>38</sup> Our

transfection data revealed that BMDM exosomes containing mostly miR-21-5p reduced Smad7 expression, suggesting that exosomal miR-21-5p could activate the TGF- $\beta$ 1 pathway in tendon by reducing Smad7 expression.

This study had some limitations. We investigated the formation of flexor tendon adhesions using a mouse model. Although the anatomy of the mouse hind paw is similar to that of zone II in the human hand,<sup>53</sup> the proposed pathway should be validated in human tissue samples. Besides, we evaluated animals at 3 weeks after surgery according to our previous study of tendon adhesion, which may be a relatively short monitoring period.

In summary, this study demonstrated a novel mechanism underlying macrophage-stromal cell communication, and it disclosed a new role of macrophage-derived exosomes in tendon adhesion. These data have multiple implications and may open new directions in clinical research. First, we suggest that targeting this mode of macrophage-tenocyte and -fibroblast communication may be a promising therapeutic strategy, providing an alternative to current treatments of traumatic tendon adhesion, which have limited efficacy. Second, specific components of exosomal cargo could be investigated as targets, including miR-21-5p and other molecules. Finally, a possibility of using macrophage-derived exosomes to deliver therapeutic agents in a tissue-specific manner may provide a potential treatment approach with limited side effects. As fibrogenesis is closely related to inflammation, it will be interesting to determine whether exosomes produced by other immune cells, such as T cells, innate lymphoid cells, basophils, and eosinophils, could regulate fibrosis during tendon repair.

## MATERIALS AND METHODS

### Animals and Macrophage Depletion

Animal protocols were approved by the Animal Research Committee of Shanghai Jiao Tong University Affiliated Sixth People's Hospital, and all procedures were performed according to the NIH Guidelines for the Care and Use of Laboratory Animals.

Clo-Lipo or PBS-Lipo (<http://www.clodronateliposomes.org>) were applied as previously described.<sup>13,14</sup> Briefly, 2 days prior to tendon surgery, 6- to 8-week-old male C57BL/6 mice were administered 1.33 mL/100 g Clo-Lipo or PBS-Lipo by intraperitoneal (i.p.) injection, and an additional 100  $\mu$ L Clo-Lipo was injected directly into the tendon at the time of surgery. Animals then received weekly injections of the same dose (1.33 mL/100 g, i.p.) until the end of the experiment.

### Flexor Tendon Surgery

Mice underwent complete transection and repair of the FDL tendon in the right hind paw as previously reported.<sup>8,54</sup> Briefly, animals were anesthetized by an i.p. injection of 4 mg/kg xylazine and 60 mg/kg ketamine. After preparation of the surgical site, the FDL was surgically transected in the transverse plane at the myotendinous junction of the calf to protect the repair site from high strain, and the skin was closed by 6-0 nylon running sutures (Ethicon, Edinburgh, UK). Then,

a 2-cm incision was made on the posterior surface of the hind paw, and soft tissue was retracted to identify the FDL, which was completely transected using micro-scissors and then repaired using 8-0 prolene sutures (Ethicon, Edinburgh, UK) in a modified Kessler pattern. The skin was closed with 6-0 nylon running sutures. Sham operation was performed on the control side using the same anesthesia and exposure protocol. However, the FDL tendon was undamaged after isolating it. All mice were returned to their cages and allowed free active motion and weight bearing following recovery from anesthesia. Mice were sacrificed 21 days after FDL tendon repair and used for analysis.

### Macroscopic Evaluation

Macroscopic evaluation was performed in five mice from each group, and peritendinous adhesions were assessed by three independent observers according to the adhesion grading system:<sup>8,9</sup> grade 1, no adhesion; grade 2, adhesion can be separated by blunt dissection alone; grade 3, sharp dissection is required to separate less than or equal to 50% of the adhesion area; grade 4, sharp dissection is required to separate 51%–97.5% of the adhesion area; and grade 5, sharp dissection is required to separate more than 97.5% of the adhesion area.

### Histological Evaluation

Mice were sacrificed and skin and excess soft tissue were removed at the mild-tibia, whereas skin on the sole of the foot remained intact so as not to disturb the repair site. Specimens were fixed for 24 hr in 4% paraformaldehyde (PFA) buffered with PBS and then decalcified in Plank-Rychlo decalcifying fluid for 14 days at room temperature. After dehydration in a graded series of ethanol and embedment in paraffin, 4- $\mu$ m sagittal slices were cut and stained with H&E and Masson's trichrome.

Histological evaluation was performed in five specimens from each group according to the histological scoring system.<sup>8,9</sup> Histologic adhesions were assessed as follows: grade 1, no adhesions; grade 2, mild (<33% of the tendon surface); grade 3, moderate (33%–66% of the tendon surface); and grade 4, severe (>66% of the tendon surface).

Histologic tendon healing was assessed as follows:<sup>8,9</sup> grade 1, good tendon continuity and smooth epitenon surface (excellent); grade 2, intratendinous collagen bundles exhibited good repair, but the epitenon was interrupted by adhesions (good); grade 3, irregularly arranged and partly broken intratendinous collagen bundles (fair); and grade 4, failed healing or massive overgrowth of granulation tissue (poor).

The sections were observed under light microscopy (Leica DM 4000 B) by two independent observers blinded to the experimental groups.

### Gliding Function Testing

Following sacrifice, the lower hind limb was detached at the knee, and the proximal FDL tendon along the tibia was isolated proximal to the tarsal tunnel without disrupting the skin at the ankle or foot. The

proximal end of the tendon was secured using cyanoacrylate between two pieces of tape, as previously described.<sup>54,55</sup> Briefly, the tibia was rigidly gripped, and the FDL tendon was incrementally loaded with small weights from 0 to 19 g; then digital images were taken at each load. The flexion angle of the MTP joint was measured from the digital images by two independent observers using ImageJ software.

### Biomechanical Analysis

Following gliding assessment, the tibia was removed at the ankle and the toes and proximal section of the FDL in the tape were mounted on the Instron 8841 DynaMight axial servohydraulic testing system (Instron) using a custom grip, as previously described.<sup>56</sup> The tendons were tested in tension at a rate of 30 mm/min until failure.

### Western Blotting Analysis

The tissue proteins were extracted from healing tendons at 21 days post-surgery. Proteins were extracted from the repair site and 1–2 mm of native tendon on both sides of the repair.

The proteins extracted from cells, tissues, and exosomes were separated by SDS-PAGE and transferred to polyvinylidene fluoride (PVDF) membranes (Millipore). Membranes were post-blocked with 5% fat-free dried milk in Tris-buffered saline for 2 hr at room temperature (RT), and they were incubated at 4°C overnight with the following: anti-CD9 (1:1,000, Abcam, ab92726), anti-CD63 (1:1,000, Abcam, ab217345), anti-TSG101 (1:1,000, Abcam, ab125011), anti-ALIX (1:1,000, Abcam, ab117600), anti-CD68 (1:1,000, Abcam, ab125212), anti-COL I (1:1,000, Abcam, ab34710), anti-COL III (1:1,000, Novus Biologicals, NBP1-05119), anti- $\alpha$ -SMA (1:1,000, Abcam, ab5694), anti-TGF- $\beta$ 1 (1:1,000, Abcam, ab64715), anti-SMAD 7 (1:1,000, Santa Cruz Biotechnology, sc-365846), anti- $\beta$ -actin (1:1,000, Abcam, ab8226), and anti-GAPDH (1:1,000, Abcam, ab8245) antibodies. Membranes were post-incubated with horseradish peroxidase (HRP)-conjugated anti-mouse or anti-rabbit immunoglobulin G (IgG) at RT for 2 hr after washing with Tris-buffered saline Tween (TBST) buffer three times, and then they were washed with TBST buffer three times again. Bands were scanned using enhanced chemiluminescence (ECL) detection system, and quantification was performed using ImageJ software.

### Cell Culture

The NIH 3T3 fibroblast cell line was purchased from Cell Bank of Type Culture Collection of the Chinese Academy of Sciences (Shanghai Institute of Cell Biology) and cultured in DMEM (Gibco) supplemented with 10% fetal bovine serum (FBS; Gibco).

Tenocytes were harvested from murine superficial flexor tendons as previously reported.<sup>8</sup> Briefly, pieces of the tendons were digested with 0.15% collagenase NB4 (SERVA Electrophoresis, Heidelberg, Germany) for 2 hr at 37°C, then the mixture was filtered through a cell mesh (Corning). After centrifugation at 300  $\times$  g for 5 min, the cell pellet was resuspended in DMEM containing 10% FBS (Gibco) and 1% penicillin-streptomycin.

BMDMs were isolated from the femurs and tibias of adult mice as described previously.<sup>57</sup> Tibias were flushed, and bone marrow cells were seeded into 10-cm<sup>2</sup> tissue culture plates and cultured in alpha MEM (minimum essential medium - alpha modification; Gibco) containing 10% FBS and 1% penicillin-streptomycin, supplemented with macrophage colony-stimulating factor (M-CSF) 10<sup>4</sup> U ml<sup>-1</sup> for 24 hr. Then BMDMs were cultured in alpha MEM containing 10% exosome-free FBS (SBI) to produce exosomes.

#### Exosome Purification, Characterization, and Labeling

After 72-hr macrophage culture, debris and dead cells in the medium were removed by centrifugation at 1,000 × *g* for 10 min and then filtered through a 0.2-mm filter. The medium was then subjected to ultracentrifugation at 100,000 × *g* for 4–6 hr at 4°C. After washing with PBS (100,000 × *g* for 20 min), the Exo-containing pellet was resuspended in PBS.

For electron microscopy, exosomes were fixed with 2% PFA and loaded on Formvar and carbon-coated copper grids. Then the grids were placed on 2% gelatin at 37°C for 20 min, rinsed with 0.15 M glycine and PBS, and the sections were blocked using 1% cold water fish-skin gelatin. Grids were viewed with an FEI Tecnai G2 spirit transmission electron microscope (FEI) and photographed using an AMT CCD camera (Advanced Microscopy Techniques).

Exosome particle size and concentration was determined using NTA with ZetaView PMX 120 (Particle Metrix).

To track exosomes, they were labeled with fluorescent dye using the PKH67 fluorescent cell linker kit (Sigma-Aldrich), according to the manufacturer's instructions. After labeling, the exosomes were washed in PBS and collected by ultracentrifugation (100,000 × *g* for 20 min) at 4°C. Then, PKH67-labeled exosomes were resuspended in PBS.

#### Exosome Treatment *In Vitro* and *In Vivo*

For *in vitro* assays, 2 μg exosomes (on the basis of protein measurement) were added to 1 × 10<sup>5</sup> recipient cells.<sup>22</sup>

As a previous study has shown that the quantity of circulating exosomes in mice is approximately 20 μg/mouse,<sup>22,58</sup> for *in vivo* treatment, 20 μg exosomes was transferred into recipient mice every 3 days via tail vein injection. Empty liposomes (FormuMax Scientific) were used in the control experiment.

#### Cell Proliferation

Cell proliferation was detected with Cell Counting Kit-8 (CCK-8, Dojindo Molecular Technologies) according to the manufacturer's instructions. Briefly, cells were plated into 96-well plates at an initial density of 5,000 cells/well and cultured for 12 hr. 12 hr later, the medium was removed, followed by the addition of 100 μL fresh medium with 2 μg exosomes contained. At the 24, 36, 48, and 72 hr of incubation time points, 10 μL CCK-8 solution was added, followed by incubation in the dark for 3 hr. Absorbance at 450 nm was

then measured using a spectrophotometric microplate reader (Bio-Rad 680). The optical density (OD) of the test wells minus the absorbance of the blank wells represented the proliferation of cells.

#### Cell Migration Assay

For the migration assay, 5 × 10<sup>4</sup> NIH 3T3 cells and tenocytes were plated in 24-well transwell plates with 8-μm inserts (Corning Life Science, Armonk, NY). The medium in inserts was free of FBS, whereas the medium out was supplemented with 10% FBS. For detecting exosome function, equal quantities of BMDM-derived exosomes were added into the inserts. After 24 hr of culture, cells were then stained with 0.1% crystal violet for 30 min, and non-migrating cells were removed. Representative fields were photographed and the number of migrated cells per field was counted.

#### Real-Time qPCR

Total RNA from cells and exosomes was extracted using the TRIzol reagent (Invitrogen), and complementary DNA was synthesized with a Reverse Transcription system (Toyobo) according to the manufacturer's instructions. PCR reactions were performed by a 7500 Realtime PCR System (Applied Biosystems). Expression data were uniformly normalized to the internal control U6, and the relative expression was calculated with the equation 2<sup>-ΔΔCT</sup>. The primer sequences used were as follows:

Col I primers: forward 5'-CCTCAGGGTATTGCTGGACAAC-3', reverse 5'-CAGAAGGACCTTGTTTGCCAGG-3';

Col III primers: forward 5'-AGCCACCTTGGTCAGTCCTA-3', reverse 5'-GTGTAGAAGGCTGTGGGCAT-3';

α-SMA primers: forward 5'-ACCATGAAGATCAAGATCATTGC-3', reverse 5'-TGTGTGCTAGAGGCAGAGC-3';

TGF-β1 primers: forward 5'-CAATTCCTGGCGATACCTCAG-3', reverse 5'-GCACAACCTCCGGTGACATCAA-3';

Smad7 primers: forward 5'-GCTCCCATCCTGTGTGTTAA-3', reverse 5'-TAGGTGTCAGCCTAGGATGGT-3';

β-actin primers: forward 5'-GCATCGTCACCAACTGGGAC-3', reverse 5'-ACCTGGCCGTCAGGCAGCTC-3';

mmu-miR-21a-5p: 5'-UAGCUUAUCAGACUGAUGUUGA-3'; and

U6 primers: forward 5'-CTCGCTTCGGCAGCACA-3', reverse 5'-AACGCTTCACGAATTTGCGT-3'.

#### Frozen Sectioning and Immunofluorescence Staining

Frozen sections from samples were prepared for immunofluorescence analyses.

Hind limbs were removed as above for harvested repaired tendon site. Heart, lungs, liver, spleen, kidney, muscle, adipose tissue, and both FDL tendons were obtained for frozen section. Tissues were fixed in PFA for 24 hr at 4°C, and they were processed in 30% sucrose (in PBS) for 24 hr prior to embedding in Cryomatrix (Thermo Fisher



Scientific, Waltham, MA). 10- $\mu$ m serial sagittal sections were cut. The primary antibody used in this study was anti-F4/80 (1:200, Abcam, ab6640). Slides were observed with an Olympus fluorescent microscope, and images were captured using an Olympus soft image viewer.

### In Situ Hybridization

Freshly frozen tendon tissue was sectioned at 10- $\mu$ m thickness using a cryostat (Leica, London, UK) and then mounted onto Superfrost Plus slides. Cryosections were fixed in 4% PFA and treated with proteinase K. The sections were acetylated with triethanolamine, acetic anhydride, and HCl and pre-hybridized in 50% formamide, 5 $\times$  saline sodium citrate, yeast tRNA, and 1 $\times$  Denhardt's solution prior to hybridization with a carboxyfluorescein (FAM)-labeled probe complementary to mouse miR-21 (LNA miRCURY probe, Exiqon, 339111YD). The probe sequence for miR-21 was 5'-TCAACAT CAGTCTGATAAGCTA-3'.

### Small RNA Deep Sequencing

Library preparation and miRNA sequencing were performed by Ribobio. Briefly, total RNA from exosomes was fractionated, and only small RNAs ranging from 18 to 30 nt were used for library preparation. After amplification by PCR, the products were sequenced using the Illumina HiSeq 2500 platform (San Diego, CA). Sequencing data supporting these studies can be found at Gene Expression Omnibus: GSE122472.

### miRNA Mimic Transfection

Fibroblasts or tenocytes ( $5 \times 10^5$ /well) were transfected with Cy3-labeled miR-21-5p mimic or control mimic (100 nmol; Ribobio, Guangzhou, China) using Lipofectamine 2000 Transfection Reagent (Invitrogen). After being cultured for 48 hr at 37°C, transfected cells were fixed with PFA for 20 min, washed, stained with Alexa Fluor 488 Phalloidin (Invitrogen), and coverslipped in Vectashield mounting medium with DAPI. Transfection efficiency (%) after 48 hr was examined using a previously reported formula:<sup>24</sup> transfection efficacy (E) = [(E/D)  $\times$  100]/X<sub>D</sub>, where D represents the number of cells used; E is the number of phalloidine cells expressing cy3-labeled miR-21-5p mimic or miRNA-mimic NC; and X<sub>D</sub> is the proliferation coefficient, which is the ratio of the number of cells on the coverslips on analysis day to those counted on transfection day.

### Lentivirus Infection

The LV-Smad7 was constructed by lentiviral vectors (GenePharma, Shanghai, China). Cell transfection was executed according to the protocol provided by the supplier. Briefly, cells were incubated in retroviral supernatant with 5  $\mu$ g/mL polybrene for 24 hr. At 48 hr after infection, cells were selected with 2.5  $\mu$ g/mL puromycin (Sigma-Aldrich) in culture medium.

### Statistical Analysis

Statistical analyses were performed using GraphPad Prism 7.0 (GraphPad, La Jolla, CA, USA). Data are expressed as mean  $\pm$  SD. The statistical significance of the differences between various groups

was calculated with Student's t tests or chi-square tests, as appropriate. p values less than 0.05 were considered statistically significant.

### AUTHOR CONTRIBUTIONS

H.C. and S.C. conducted the experiments. Y.H. and D.Z. performed the statistical analysis and the mechanical analyses. H.C. and Y.H. wrote the manuscript. Y.Y. and C.F. conceived the study and participated in its design and coordination. C.F. obtained funding and supervised the experiments. All authors read and approved the final manuscript.

### CONFLICTS OF INTEREST

The authors declare no competing interests.

### ACKNOWLEDGMENTS

This work is supported by the National Natural Science Foundation of China (81672146). We would like to thank Dr. Yue Lv for technical assistance.

### REFERENCES

1. Millar, N.L., Gilchrist, D.S., Akbar, M., Reilly, J.H., Kerr, S.C., Campbell, A.L., Murrell, G.A., Liew, F.Y., Kurowska-Stolarska, M., and McInnes, I.B. (2015). MicroRNA29a regulates IL-33-mediated tissue remodelling in tendon disease. *Nat. Commun.* 6, 6774.
2. Wang, X., Xie, L., Crane, J., Zhen, G., Li, F., Yang, P., Gao, M., Deng, R., Wang, Y., Jia, X., et al. (2018). Aberrant TGF- $\beta$  activation in bone tendon insertion induces enthesopathy-like disease. *J. Clin. Invest.* 128, 846–860.
3. Wynn, T.A., and Ramalingam, T.R. (2012). Mechanisms of fibrosis: therapeutic translation for fibrotic disease. *Nat. Med.* 18, 1028–1040.
4. Zhou, Y.L., Yang, Q.Q., Yan, Y.Y., Zhu, C., Zhang, L., and Tang, J.B. (2018). Localized delivery of miRNAs targets cyclooxygenases and reduces flexor tendon adhesions. *Acta Biomater.* 70, 237–248.
5. Sharma, P., and Maffulli, N. (2005). Tendon injury and tendinopathy: healing and repair. *J. Bone Joint Surg. Am.* 87, 187–202.
6. Docheva, D., Müller, S.A., Majewski, M., and Evans, C.H. (2015). Biologics for tendon repair. *Adv. Drug Deliv. Rev.* 84, 222–239.
7. Shalomon, K.T., Sheu, C., Chen, C.H., Chen, S.H., Jose, G., Kuo, C.Y., and Chen, J.P. (2018). Multi-functional electrospun antibacterial core-shell nanofibrous membranes for prolonged prevention of post-surgical tendon adhesion and inflammation. *Acta Biomater.* 72, 121–136.
8. Chen, S., Jiang, S., Zheng, W., Tu, B., Liu, S., Ruan, H., and Fan, C. (2017). RelA/p65 inhibition prevents tendon adhesion by modulating inflammation, cell proliferation, and apoptosis. *Cell Death Dis.* 8, e2710.
9. Jiang, S., Zhao, X., Chen, S., Pan, G., Song, J., He, N., Li, F., Cui, W., and Fan, C. (2014). Down-regulating ERK1/2 and SMAD2/3 phosphorylation by physical barrier of celecoxib-loaded electrospun fibrous membranes prevents tendon adhesions. *Biomaterials* 35, 9920–9929.
10. Stolk, M., Klatter-Schulz, F., Schmock, A., Minkwitz, S., Wildemann, B., and Seifert, M. (2017). New insights into tenocyte-immune cell interplay in an in vitro model of inflammation. *Sci. Rep.* 7, 9801.
11. Millar, N.L., Murrell, G.A.C., and McInnes, I.B. (2017). Inflammatory mechanisms in tendinopathy - towards translation. *Nat. Rev. Rheumatol.* 13, 110–122.
12. Dakin, S.G., Martinez, F.O., Yapp, C., Wells, G., Oppermann, U., Dean, B.J., Smith, R.D., Whewey, K., Watkins, B., Roche, L., and Carr, A.J. (2015). Inflammation activation and resolution in human tendon disease. *Sci. Transl. Med.* 7, 311ra173.
13. Hays, P.L., Kawamura, S., Deng, X.H., Dagher, E., Mithoefer, K., Ying, L., and Rodeo, S.A. (2008). The role of macrophages in early healing of a tendon graft in a bone tunnel. *J. Bone Joint Surg. Am.* 90, 565–579.

14. de la Durantaye, M., Piette, A.B., van Rooijen, N., and Frenette, J. (2014). Macrophage depletion reduces cell proliferation and extracellular matrix accumulation but increases the ultimate tensile strength of injured Achilles tendons. *J. Orthop. Res.* 32, 279–285.
15. Chamberlain, C.S., Leiferman, E.M., Frisch, K.E., Wang, S., Yang, X., van Rooijen, N., Baer, G.S., Brickson, S.L., and Vanderby, R. (2011). The influence of macrophage depletion on ligament healing. *Connect. Tissue Res.* 52, 203–211.
16. Blomgran, P., Blomgran, R., Ernerudh, J., and Aspenberg, P. (2016). A possible link between loading, inflammation and healing: Immune cell populations during tendon healing in the rat. *Sci. Rep.* 6, 29824.
17. Pitt, J.M., Kroemer, G., and Zitvogel, L. (2016). Extracellular vesicles: masters of intercellular communication and potential clinical interventions. *J. Clin. Invest.* 126, 1139–1143.
18. Zhang, J., Li, S., Li, L., Li, M., Guo, C., Yao, J., and Mi, S. (2015). Exosome and exosomal microRNA: trafficking, sorting, and function. *Genomics Proteomics Bioinformatics* 13, 17–24.
19. Hulsmans, M., and Holvoet, P. (2013). MicroRNA-containing microvesicles regulating inflammation in association with atherosclerotic disease. *Cardiovasc. Res.* 100, 7–18.
20. Zhang, L., Zhang, S., Yao, J., Lowery, F.J., Zhang, Q., Huang, W.C., Li, P., Li, M., Wang, X., Zhang, C., et al. (2015). Microenvironment-induced PTEN loss by exosomal microRNA primes brain metastasis outgrowth. *Nature* 527, 100–104.
21. Thomou, T., Mori, M.A., Dreyfuss, J.M., Konishi, M., Sakaguchi, M., Wolfrum, C., Rao, T.N., Winnay, J.N., Garcia-Martin, R., Grinspoon, S.K., et al. (2017). Adipose-derived circulating miRNAs regulate gene expression in other tissues. *Nature* 542, 450–455.
22. Ying, W., Riopel, M., Bandyopadhyay, G., Dong, Y., Birmingham, A., Seo, J.B., Ofrecio, J.M., Wollam, J., Hernandez-Carretero, A., Fu, W., et al. (2017). Adipose Tissue Macrophage-Derived Exosomal miRNAs Can Modulate In Vivo and In Vitro Insulin Sensitivity. *Cell* 171, 372–384.e12.
23. Wang, C., Zhang, C., Liu, L., A, X., Chen, B., Li, Y., and Du, J. (2017). Macrophage-Derived mir-155-Containing Exosomes Suppress Fibroblast Proliferation and Promote Fibroblast Inflammation during Cardiac Injury. *Mol. Ther.* 25, 192–204.
24. Simeoli, R., Montague, K., Jones, H.R., Castaldi, L., Chambers, D., Kelleher, J.H., Vacca, V., Pitcher, T., Grist, J., Al-Ahdal, H., et al. (2017). Exosomal cargo including microRNA regulates sensory neuron to macrophage communication after nerve trauma. *Nat. Commun.* 8, 1778.
25. Bartel, D.P. (2004). MicroRNAs: genomics, biogenesis, mechanism, and function. *Cell* 116, 281–297.
26. Dakin, S.G. (2017). MicroRNA Replacement: A New Era of Molecular Therapy for Tendon Disorders? *Mol. Ther.* 25, 2243–2244.
27. Usman, M.A., Nakasa, T., Shoji, T., Kato, T., Kawanishi, Y., Hamanishi, M., Kamei, N., and Ochi, M. (2015). The effect of administration of double stranded MicroRNA-210 on acceleration of Achilles tendon healing in a rat model. *J. Orthop. Sci.* 20, 538–546.
28. Chen, Q., Lu, H., and Yang, H. (2014). Chitosan inhibits fibroblasts growth in Achilles tendon via TGF- $\beta$ 1/Smad3 pathway by miR-29b. *Int. J. Clin. Exp. Pathol.* 7, 8462–8470.
29. Lu, Y.F., Liu, Y., Fu, W.M., Xu, J., Wang, B., Sun, Y.X., Wu, T.Y., Xu, L.L., Chan, K.M., Zhang, J.F., and Li, G. (2017). Long noncoding RNA H19 accelerates tenogenic differentiation and promotes tendon healing through targeting miR-29b-3p and activating TGF- $\beta$ 1 signaling. *FASEB J.* 31, 954–964.
30. Watts, A.E., Millar, N.L., Platt, J., Kitson, S.M., Akbar, M., Rech, R., Griffin, J., Pool, R., Hughes, T., McInnes, L.B., and Gilchrist, D.S. (2017). MicroRNA29a Treatment Improves Early Tendon Injury. *Mol. Ther.* 25, 2415–2426.
31. Dubin, J.A., Greenberg, D.R., Iglinski-Benjamin, K.C., and Abrams, G.D. (2018). Effect of micro-RNA on tenocytes and tendon-related gene expression: A systematic review. *J. Orthop. Res.* Published online June 6, 2018. <https://doi.org/10.1002/jor.24064>.
32. Pottier, N., Cauffiez, C., Perrais, M., Barbry, P., and Mari, B. (2014). FibromiRs: translating molecular discoveries into new anti-fibrotic drugs. *Trends Pharmacol. Sci.* 35, 119–126.
33. Chau, B.N., Xin, C., Hartner, J., Ren, S., Castano, A.P., Linn, G., Li, J., Tran, P.T., Kaimal, V., Huang, X., et al. (2012). MicroRNA-21 promotes fibrosis of the kidney by silencing metabolic pathways. *Sci. Transl. Med.* 4, 121ra18.
34. Thum, T., Gross, C., Fiedler, J., Fischer, T., Kissler, S., Bussen, M., Galuppo, P., Just, S., Rottbauer, W., Frantz, S., et al. (2008). MicroRNA-21 contributes to myocardial disease by stimulating MAP kinase signalling in fibroblasts. *Nature* 456, 980–984.
35. Liu, G., Friggeri, A., Yang, Y., Milosevic, J., Ding, Q., Thannickal, V.J., Kaminski, N., and Abraham, E. (2010). miR-21 mediates fibrogenic activation of pulmonary fibroblasts and lung fibrosis. *J. Exp. Med.* 207, 1589–1597.
36. Ardite, E., Perdiguerro, E., Vidal, B., Gutarra, S., Serrano, A.L., and Muñoz-Cánoves, P. (2012). PAI-1-regulated miR-21 defines a novel age-associated fibrogenic pathway in muscular dystrophy. *J. Cell Biol.* 196, 163–175.
37. Pakshir, P., and Hinz, B. (2018). The big five in fibrosis: Macrophages, myofibroblasts, matrix, mechanics, and miscommunication. *Matrix Biol.* 68–69, 81–93.
38. Zhou, Y., Zhang, L., Zhao, W., Wu, Y., Zhu, C., and Yang, Y. (2013). Nanoparticle-mediated delivery of TGF- $\beta$ 1 miRNA plasmid for preventing flexor tendon adhesion formation. *Biomaterials* 34, 8269–8278.
39. Johnnidis, J.B., Harris, M.H., Wheeler, R.T., Stehling-Sun, S., Lam, M.H., Kirak, O., Brummelkamp, T.R., Fleming, M.D., and Camargo, F.D. (2008). Regulation of progenitor cell proliferation and granulocyte function by microRNA-223. *Nature* 451, 1125–1129.
40. Théry, C., Zitvogel, L., and Amigorena, S. (2002). Exosomes: composition, biogenesis and function. *Nat. Rev. Immunol.* 2, 569–579.
41. Cavarretta, E., and Condorelli, G. (2015). miR-21 and cardiac fibrosis: another brick in the wall? *Eur. Heart J.* 36, 2139–2141.
42. McClelland, A.D., Herman-Edelstein, M., Komers, R., Jha, J.C., Winbanks, C.E., Hagiwara, S., Gregorevic, P., Kantharidis, P., and Cooper, M.E. (2015). miR-21 promotes renal fibrosis in diabetic nephropathy by targeting PTEN and SMAD7. *Clin. Sci. (Lond.)* 129, 1237–1249.
43. Ismail, N., Wang, Y., Dakhlallah, D., Moldovan, L., Agarwal, K., Batte, K., Shah, P., Wisler, J., Eubank, T.D., Tridandapani, S., et al. (2013). Macrophage microvesicles induce macrophage differentiation and miR-223 transfer. *Blood* 121, 984–995.
44. Millar, N.L., Hueber, A.J., Reilly, J.H., Xu, Y., Fazzi, U.G., Murrell, G.A., and McInnes, I.B. (2010). Inflammation is present in early human tendinopathy. *Am. J. Sports Med.* 38, 2085–2091.
45. Marsolais, D., Côté, C.H., and Frenette, J. (2001). Neutrophils and macrophages accumulate sequentially following Achilles tendon injury. *J. Orthop. Res.* 19, 1203–1209.
46. Yuan, D., Zhao, Y., Banks, W.A., Bullock, K.M., Haney, M., Batrakova, E., and Kabanov, A.V. (2017). Macrophage exosomes as natural nanocarriers for protein delivery to inflamed brain. *Biomaterials* 142, 1–12.
47. Mendias, C.L., Gumucio, J.P., and Lynch, E.B. (2012). Mechanical loading and TGF- $\beta$  change the expression of multiple miRNAs in tendon fibroblasts. *J. Appl. Physiol.* (1985) 113, 56–62.
48. Wang, B., Guo, J., Feng, L., Suen, C.W., Fu, W.M., Zhang, J.F., and Li, G. (2016). MiR124 suppresses collagen formation of human tendon derived stem cells through targeting egr1. *Exp. Cell Res.* 347, 360–366.
49. Li, C.X., Talele, N.P., Boo, S., Koehler, A., Knee-Walden, E., Balestrini, J.L., Speight, P., Kapus, A., and Hinz, B. (2017). MicroRNA-21 preserves the fibrotic mechanical memory of mesenchymal stem cells. *Nat. Mater.* 16, 379–389.
50. Chen, S.Y., Shiau, A.L., Wu, C.L., and Wang, C.R. (2016). Intraarticular overexpression of Smad7 ameliorates experimental arthritis. *Sci. Rep.* 6, 35163.
51. Feagan, B.G., Sands, B.E., Rossiter, G., Li, X., Usiskin, K., Zhan, X., and Colombel, J.F. (2018). Effects of Mongersen (GED-0301) on Endoscopic and Clinical Outcomes in Patients With Active Crohn's Disease. *Gastroenterology* 154, 61–64.e6.
52. Zheng, W., Song, J., Zhang, Y., Chen, S., Ruan, H., and Fan, C. (2017). Metformin prevents peritendinous fibrosis by inhibiting transforming growth factor- $\beta$  signaling. *Oncotarget* 8, 101784–101794.

53. Wong, J., Bennett, W., Ferguson, M.W.J., and McGrouther, D.A. (2006). Microscopic and histological examination of the mouse hindpaw digit and flexor tendon arrangement with 3D reconstruction. *J. Anat.* 209, 533–545.
54. Loisel, A.E., Bragdon, G.A., Jacobson, J.A., Hasslund, S., Cortes, Z.E., Schwarz, E.M., Mitten, D.J., Awad, H.A., and O’Keefe, R.J. (2009). Remodeling of murine intrasynovial tendon adhesions following injury: MMP and neotendon gene expression. *J. Orthop. Res.* 27, 833–840.
55. Ackerman, J.E., Best, K.T., O’Keefe, R.J., and Loisel, A.E. (2017). Deletion of EP4 in S100a4-lineage cells reduces scar tissue formation during early but not later stages of tendon healing. *Sci. Rep.* 7, 8658.
56. Ackerman, J.E., and Loisel, A.E. (2016). Murine Flexor Tendon Injury and Repair Surgery. *J. Vis. Exp.* 115, 1–14.
57. Ying, W., Cheruku, P.S., Bazer, F.W., Safe, S.H., and Zhou, B. (2013). Investigation of macrophage polarization using bone marrow derived macrophages. *J. Vis. Exp.* (76), 50323.
58. Li, J., Zhang, Y., Liu, Y., Dai, X., Li, W., Cai, X., Yin, Y., Wang, Q., Xue, Y., Wang, C., et al. (2013). Microvesicle-mediated transfer of microRNA-150 from monocytes to endothelial cells promotes angiogenesis. *J. Biol. Chem.* 288, 23586–23596.